Bioorganic Chemistry 91 (2019) 103112

Contents lists available at ScienceDirect

Bioorganic Chemistry

journal homepage: www.elsevier.com/locate/bioorg

Synthesis of new arylhydrazide bearing Schiff bases/thiazolidinone: α-Amylase, urease activities and their molecular docking studies

Fazal Rahim[a,*], Muhammad Taha[b,*], Hayat Ullah[a], Abdul Wadood[c], Manikandan Selvaraj[d], Abdur Rab[a], Muhammad Sajid[e], Syed Adnan Ali Shah[f,g], Nizam Uddin[h], Mohammed Gollapalli[i]

[a] Department of Chemistry, Hazara University, Mansehra 21300, Khyber Pakhtunkhwa, Pakistan
[b] Department of Clinical Pharmacy, Institute for Research and Medical Consultations (IRMC), Imam Abdulrahman Bin Faisal University, P.O. Box 1982, Dammam 31441, Saudi Arabia
[c] Department of Biochemistry, Abdul Wali Khan University Mardan, Mardan 23200, Pakistan
[d] Monash University School of Chemical Engineering, Bandar Subway, 47500 Selangor Alam Campus, 42300, Malaysia
[e] Department of Biochemistry, Hazara University, Mansehra 21300, Khyber Pakhtunkhwa, Pakistan
[f] Atta-ur-Rahman Institute for Natural Products Discovery (AuRIns), Universiti Teknologi MARA Cawangan Selangor Kampus Puncak Alam, 42300 Bandar Puncak Alam, Selangor D. E., Malaysia.
[g] Faculty of Pharmacy, Universiti Teknologi MARA Cawangan Selangor Kampus Puncak Alam, 42300 Bandar Puncak Alam, Selangor D. E., Malaysia
[h] Department of Chemistry, University of Karachi, Karachi 75270, Pakistan
[i] Department of Computer Information Systems, College of Computer Science & Information Technology (CCSIT), Imam Abdulrahman Bin Faisal University, P.O. Box 1982, Dammam 31441, Saudi Arabia

ARTICLE INFO

Keywords:
Synthesis
Arylhydrazide
Schiff bases
Thiazolidinone
α-Amylase
Urease
Molecular docking
Structure activity relationship

ABSTRACT

Alpha-amylase and urease enzyme over expression endorses various complications like rheumatoid arthritis, urinary tract infection, colon cancer, metabolic disorder, cardiovascular risk, and chronic kidney disease. To overcome these complications, we have synthesized new arylhydrazide bearing Schiff bases/thiazolidinone analogues as α-amylase and urease inhibitors. The analogues **1a-r** were evaluated for α-amylase inhibitory potential. All analogues were found active and show IC_{50} value ranging between 0.8 ± 0.05 and 12.50 ± 0.5 μM as compare to standard acarbose (IC_{50} = 1.70 ± 0.10 μM). Among the synthesized analogs, compound **1j**, **1r**, **1k**, **1e**, **1b** and **1f** having IC_{50} values 0.8 ± 0.05, 0.9 ± 0.05, 1.00 ± 0.05, 1.10 ± 0.10, 1.20 ± 0.10 and 1.30 ± 0.10 μM respectively showed an excellent inhibitory potential. Analogs **2a-o** were evaluated against urease activity. All analogues were found active and show IC_{50} value ranging between 4.10 ± 0.02 and 38.20 ± 1.10 μM as compare to standard thiourea (IC_{50} = 21.40 ± 0.21 μM). Among the synthesized analogs, compound **2k**, **2a**, **2h**, **2j**, **2f**, **2e**, **2g**, **2b** and **2l** having IC_{50} values 4.10 ± 0.02, 4.60 ± 0.02, 4.70 ± 0.03, 5.40 ± 0.02, 6.70 ± 0.05, 8.30 ± 0.3, 11.20 ± 0.04, 16.90 ± 0.8 and 19.80 ± 0.60 μM respectively showed an excellent inhibitory potential. All compounds were characterized through ^{1}H, ^{13}C NMR and HR-EIMS analysis. Structure activity relationship of the synthesized analogs were recognized and confirmed through molecular docking studies.

1. Introduction

In modern drug discovery research, an enzyme inhibition plays a vital role. Urease and α-amylase are two vital enzymes that are closely associated with different clinical conditions. α-Amylase inhibition effectively showed the reduction of glucose bioavailability [1]. In order to control the hyperglycemia of diabetic type-2 patients, this phenomenon is considered as an important strategy [2]. In 21st century, it is anticipated that type-2 diabetes is considered as one of the major human health concerns [3]. Herein, most effective, cheaper and safer α-amylase inhibitors needed to be discovered. α-Amylase synthetic inhibitors are commercially available but these marketed drugs cause side effects [4]. *Helicobacter pylori* are responsible for gastrointestinal ulcers that produce urease as mechanism to survive in acidic environment of stomach. World widely, it has been estimated that 50% of world population is infected by *H-pylori* [5]. According to this particular to cure the stomach ulcer, the urease inhibition can lead to get rid the H-pylori infections [6,7]. Urease inhibitors play a vital role to depress the microbial urease potential that converts the urea fertilizers into ammonia that leads to the great environmental and economic losses [8].

* Corresponding authors.
E-mail addresses: fazalstar@gmail.com (F. Rahim), mtaha@iau.edu.sa (M. Taha).

https://doi.org/10.1016/j.bioorg.2019.103112
Received 21 April 2019; Received in revised form 9 June 2019; Accepted 7 July 2019
Available online 09 July 2019

Besides synthetic heterocyclic analogues, some important medicinal plants like hypericum lanuginosum, aegle marmelos, juglans regia, cistanche phelypaea, heracleum sphondylium and Ipomoea batatas have showed broad spectrum biological potentials as anti-diabetic, antioxidant and anti-inflammatory, etc. [9–14].

Hydrazide scaffold are important nitrogen containing molecule that show anti-cancer [15], anti-malarial [16], anti-inflammatory [17], anti-viral [18], anti-bacterial [19], anti-fungal [20] activities. Among these biologically potent hydrazide scaffolds, aryl-hydrazide scaffolds have recently attracted wonderful interest from chemist due to their outstanding potentials [21]. Thiazolidinone is known to have a varied range of biological potentials such as anti-bacterial [22], anti-fungal [23], anti-viral [24], anti-inflammatory [25] and anti-tuberculosis [26], etc. Our research group had already reported hydrazide-based Schiff bases [27], benzofuran based hydrazone [28], 3,4-dimethoxy benzohydrazide [29], 4-thiazolidinone analogs [30] as *α*-amylase and urease inhibitors. Here in this present study, we are going to report the synthesis of arylhydrazide bearing Schiff bases/thiazolidinone that showed much more potency against *α*-amylase and urease enzymes as compare to standard drugs. The compounds were synthesized by simple modes of synthesis like amide formation, Schiff base formation and heterocyclic ring formation [31] (see Fig. 1).

2. Results and discussion

2.1. Chemistry

We reacted and reflux hydrazine hydrate with 4-cyanobezoate to give aryl hydrazide as intermediate product (**I**). Synthesized intermediate (**I**) was used in two different ways. Firstly, intermediate (**I**) was reacted and refluxed with different substituted aldehydes/acetophenone to give arylhydrazide bearing Schiff bases products **(1–18)** (Scheme-1: **1a-r**). Secondly, Schiff bases products were refluxed with thioglycolic acid to give arylhydrazide bearing thiazolidinone product **(1–15)**. The products were confirmed through ^{1}H, ^{13}C NMR and HR-EIMS analysis (Scheme-2: **2a-o**) Table 1.

2.2. α-Amylase activity of arylhydrazide bearing Schiff bases

Our group is working on enzyme inhibitions [32] to developed novel inhibitors. We have synthesized nineteen analogues of arylhydrazide bearing Schiff bases (**1a-r**) showed varied degree of potential against α-amylase enzyme with IC_{50} value ranging between (0.8 ± 0.05–12.50 ± 0.5 μM). Analogs **1j**, **1r**, **1k**, **1e**, **1b** and **1f** having IC_{50} values 0.8 ± 0.05, 0.9 ± 0.05, 1.00 ± 0.05, 1.10 ± 0.10, 1.20 ± 0.10, and 1.30 ± 0.10 showed many folds better potency as compare to standard acarbose (IC_{50} = 1.70 ± 0.10 μM). The dichloro substituted analog **1j** showed better potency as compare to the monochloro substituted analog **1a**. Nitro substituted analog **1c** (*ortho* substituted analog) and **1l** (*para* substituted analog) showed IC_{50} value 1.70 ± 0.10 and 1.90 ± 0.10 μM. It was observed that presence of polar group on phenyl ring at different position mainly effect the inhibitory potential.

2.3. Docking studies of arylhydrazide bearing Schiff bases

Using Gold molecular docking software, the synthesized arylhydrazide bearing Schiff bases derivatives were docked into the active site of the target enzyme Amylase (pdb: 4W93). The main interactions recognized by active compounds were inside the 4Å radius on the binding site of amylase, were deliberated as most dominant factor for the activity. Almost all compounds **(1a-r)** in this series were active with IC_{50} value ranging 0.80 ± 0.05–12.30 ± 0.50 μM. Here we describe the binding site of four most potent compounds (**1j**, **1r**, **1k** and **1e**). Interactive site of the standard drug acarbose had been described in our article [33].

The Compound **1j** is the most active scaffold in this series and the binding site shows that the hydroxyl moieties attached *meta* and *para* position of the benzene ring forms hydrogen bonds to GLU233 and in addition the GLN63 forms hydrogen bond to methylidene group. Additionally, the TRP59 indole ring forms π-π stacking with isocyano phenyl ring. TYR151 and HIS201, also the benzodiazolyl ring forms π-π stacking with TRY62, respectively (Fig. 2a).

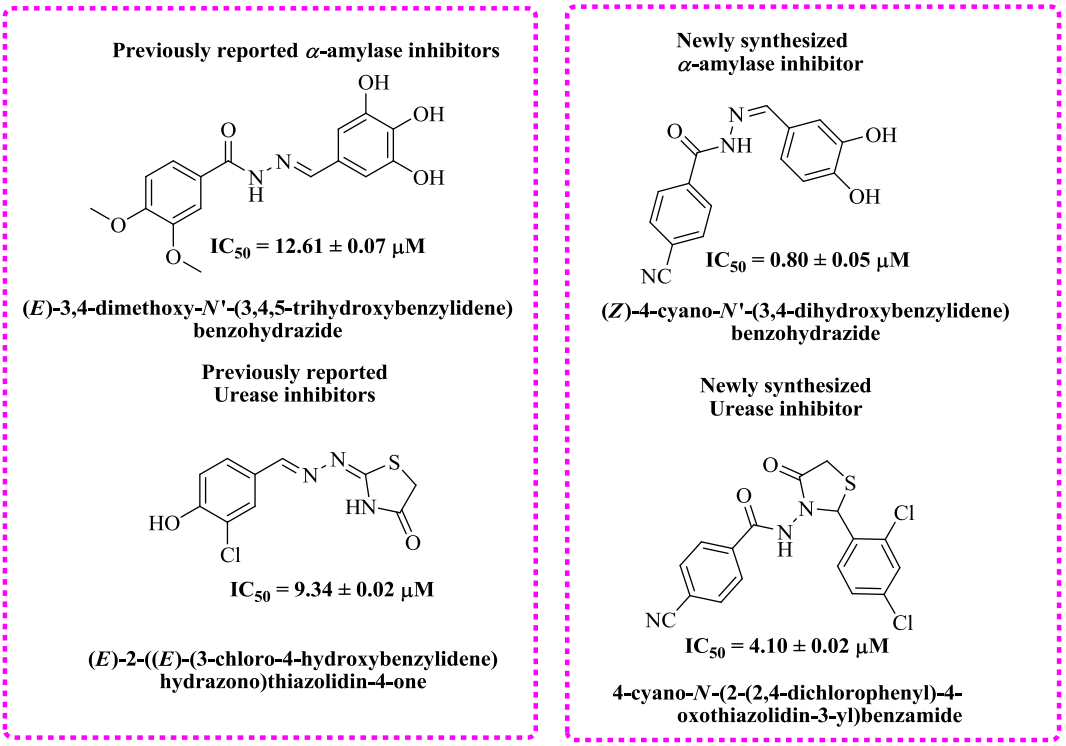

Fig. 1. Comparison of newly synthesized arylhydrazide Schiff base/thiazolidinone with previously reported scaffolds.

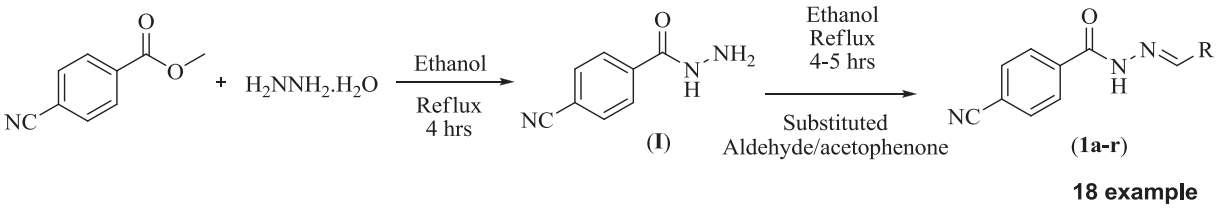

Scheme 1. Synthesis of arylhydrazide Schiff bases.

Fig. 2b show the binding site of the compound **1r**, the GLN63 forms hydrogen bonds to methylidene group of the compound **1r**. Additionally, the TRP59 indole ring forms π-π stacking with isocyano phenyl ring. HIS201 and TYR151, also the benzodiazolyl ring forms π-π stacking with TYR62, correspondingly. Apart from these interactions there is also hydrophobic interaction established by ALA198 side chain.

Fig. 2c represent the binding site of the scaffold **1k**, a hydrogen bond is established between GLU233 and NH group attached to the phenyl of the compound **1k**. Additionally, the TRP59 indole ring forms π-π stacking with isocyano phenyl ring of the compound. In addition to the normal hydrogen bonding, Carbon Hydrogen Bond is formed between HIS305 and nitrile group of the compound. Likewise, π-donor hydrogen bond is observed between ASP197 and π-orbitals of the benzene ring of compound **1k**.

Finally, the binding site orientation of the scaffold **1e** show the establishment of hydrogen bond of compound **1e** Phenol hydroxyl group with GLU233 side chain and a π-donor hydrogen bond is observed between ASP197 and π-orbitals of the benzene ring of compound **1e** and carbon hydrogen bond is formed between HIS305 and nitrile group of the compound. The isocyano phenyl ring forms π-π stacking with TRP59 indole ring (Fig. 2d). In general docking studies showed that the presence isocyano phenyl ring of this series forms π- π stacking with TRP59 and the presence of the polar group at the *meta* or *para* position on the phenyl ring was influential in forming hydrogen bond that stabilize the complex and reflects in the biological activity index.

2.4. Urease activity of arylhydrazide bearing thiazolidinone

Synthesized **15** analogs of arylhydrazide bearing thiazolidinone (**2a-o**) showed varied degree of potential against Urease inhibitory potential with IC_{50} value ranging between 4.10 ± 0.02 and 38.20 ± 1.10 μM. Analogs **2k, 2a**, **2h**, **2j**, **2f, 2e**, **2g**, **2b** and **2l** having IC_{50} values 4.10 ± 0.02, 4.60 ± 0.02, 4.70 ± 0.03, 5.40 ± 0.02, 6.70 ± 0.05, 8.30 ± 0.3, 11.20 ± 0.04, 16.90 ± 0.8 and 19.80 ± 0.60 showed many fold better potency as compare to standard thiourea (IC_{50} = 21.40 ± 0.21 μM).

Analog **2k** was the most potent analog among the synthesized analogs. The presence of two chloro group at *ortho* and *para* position might be responsible for the highest potency. Analog **2a** was the second most potent analog which might me due to the presence of *para* chloro as substituent. The nitro substituted analogs **2h**, **2f** and **2e** (*ortho*, *para* and *meta* respectively) having IC_{50} value 4.70 ± 0.03, 6.70 ± 0.05 and 8.30 ± 0.3 showed excellent potency. The *ortho* substituted analog showed an excellent potency as compare to *para* and *meta* substituted one. It was observed that the *meta* substituted analog was the least one as compares to *ortho* and *para* analogs. The dimethyl substituted analogs **2i** and **2n** showed IC_{50} value 22.20 ± 0.60 and 28.20 ± 0.60 μM. It was observed that 2,3-dimethyl substituted analogs showed good inhibitory potential as compare to the 2,4-dimethyl substituted analog. In case of **2b** (3-bromo-5-methoxy) and **2o** (2-bromo-4-methoxy) substituted analogs showed inhibitory potential with IC_{50} value 16.90 ± 0.8 and 38.20 ± 1.10 μM.

2.5. Docking studies of arylhydrazide bearing thiazolidinone

Molecular docking study was conducted using the default parameters implemented in MOE modeling package, in order to explore the binding pattern of all the synthesized thiazolidinone derivatives (**2a-o**) with in the active site of the crystal structure of urease enzyme. Active site of the urease enzyme comprises of both hydrophilic and hydrophobic amino acids. The hydrophilic site included G166, 223, R339, D224, 494, H 315, 323, 324, and 249, while the hydrophobic site was composed of A170, 366, K169, L319, and C322. Additionally, this enzyme carried one modified tyrosine residues (KCX-220), and two nickel (Ni) ions in their active cavity, which can jointly compete a significant role by linking key amino acid with ligands, and further trigger the urease activity. However, the foremost favorable docking conformations of all the derivatives were ascertained within the active site with proper orientation. Consequently, from the docking study, it has been observed that all the derivatives showed fit-well pattern of binding within the active site pocket of the corresponding enzyme. Next, the most promising docked conformation of each compound was further evaluated for PL analysis, based on the standard protocol implemented in MOE-docking contents, i.e., the GBVI/WSA binding free energy calculation. Subsequently, it has been observed that all the synthesized derivatives carry various substituted groups at benzene ring (i.e., electron withdrawing (EWG), and donating (EDG) groups), hence, this variation in groups, their quantity, and its position eventually impact the urease activity. In case of the most active derivative **2k** (4.10 ± 0.02) in the series showed fit-well pattern of binding in the active site of the urease enzyme, this compound carries EWG (di-chloro) at *para* and *ortho* position over benzene ring. The deep PL interaction pose analysis for this compound **2k** showed fit-well pattern of binding in the active site and adopt most favorable ionic and other interactions (i.e. hydrogen bond, hydrophobic, etc.) with the catalytic residues, such as H323, R339, M367, and with the modified residue KCX-220. Additionally, the two embedded ions (Ni-798 & 799) in the active pocket adopt ionic bond with the O^{10} and O^{8} of the corresponding

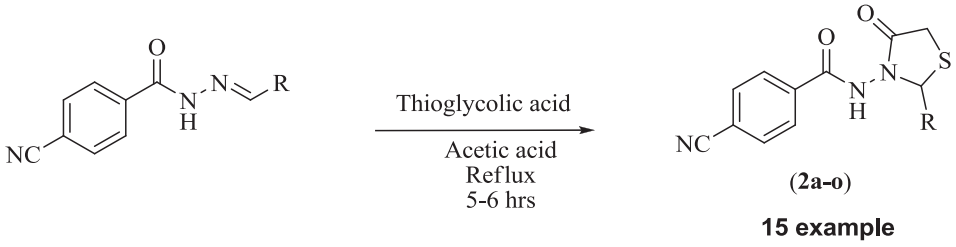

Scheme 2. Synthesis of arylhydrazide bearing thiazolidinone.

Table 1
Structure of synthesized arylhydrazide bearing Schiff bases/thiazolidinone.

S. No	R	S. No	R
1a	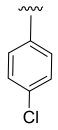	**2a**	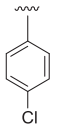
1b	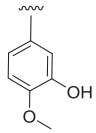	**2b**	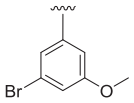
1c	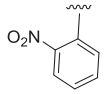	**2c**	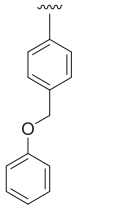
1d	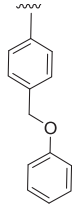	**2d**	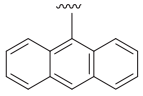
1e	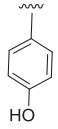	**2e**	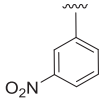
1f	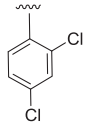	**2f**	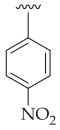
1g	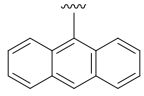	**2g**	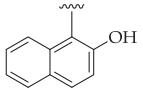
1h	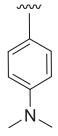	**2h**	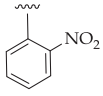
1i	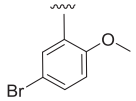	**2i**	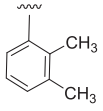
1j	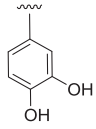	**2j**	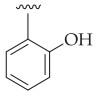
1k	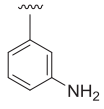	**2k**	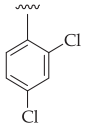

Table 1 (*continued*)

S. No	R	S. No	R
1l	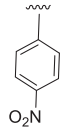	**2l**	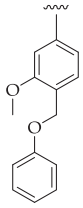
1m	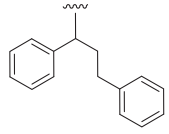	**2m**	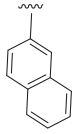
1n	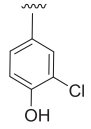	**2n**	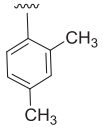
1o	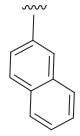	**2o**	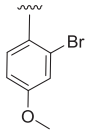
1p	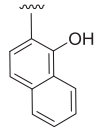		
1q	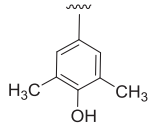		
1r	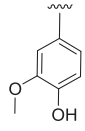		

compound, and further enhance the activity against urease enzyme. The high potency of this compound might be due to the attached EWG quantity at the benzene ring which further fully stabilized the ring. Other reason about the high potency might be due to the ionic interaction with both the Ni ions and as well as with the modified lysine residue, which play important role in enhancing the activity against the urease enzyme as shown in Fig. 3b. In case of other compounds whose possess single EWG, subsequently withdraw electron from this benzene ring through inductive effect, and remain the benzene ring partial +ve, so this ring further adopts pi-stacking interaction with other groups to regain stabilization state.

Furthermore, in case of other active compounds that includes **2a**, **2h**, **2f**, **2e**, etc., in the series showed good activity against urease enzyme. In case of 2nd active compound **2a** (**4.60 ± 0.02**) in the series further demonstrate the inhibition pattern in term of adopting various interaction with the catalytic residues, i.e., R339, M367, and with the modified lysine residues KCX-220, additionally, the Ni799 adopted ionic interaction with the O^{21} of the compound. The high potency of this compound is might be due the EWG inductive effect, and unable

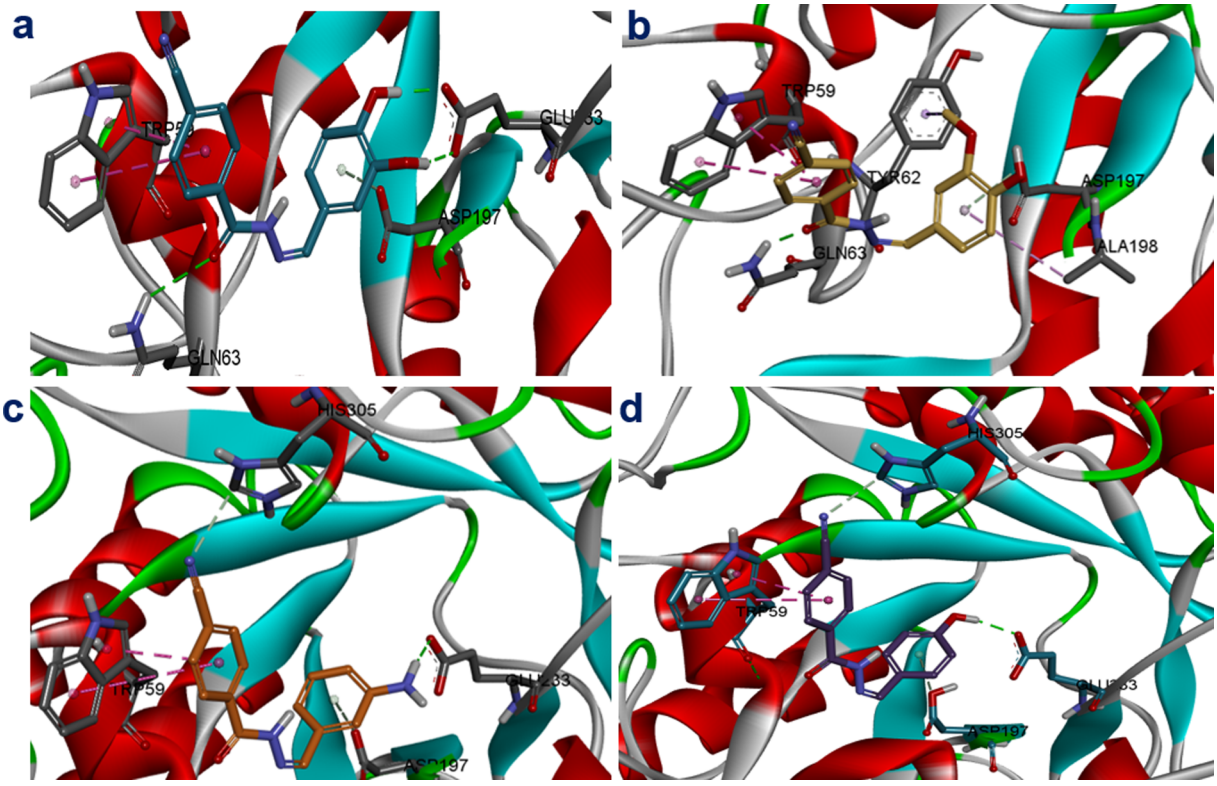

Fig. 2. Show the binding mode of the active compounds in the *α*-amylase active site (a) compound **1j** in blue stick, (b) compound **1r** in pale brown stick (c) compound **1k** in brown stick and (d) compound **1e** green stick.

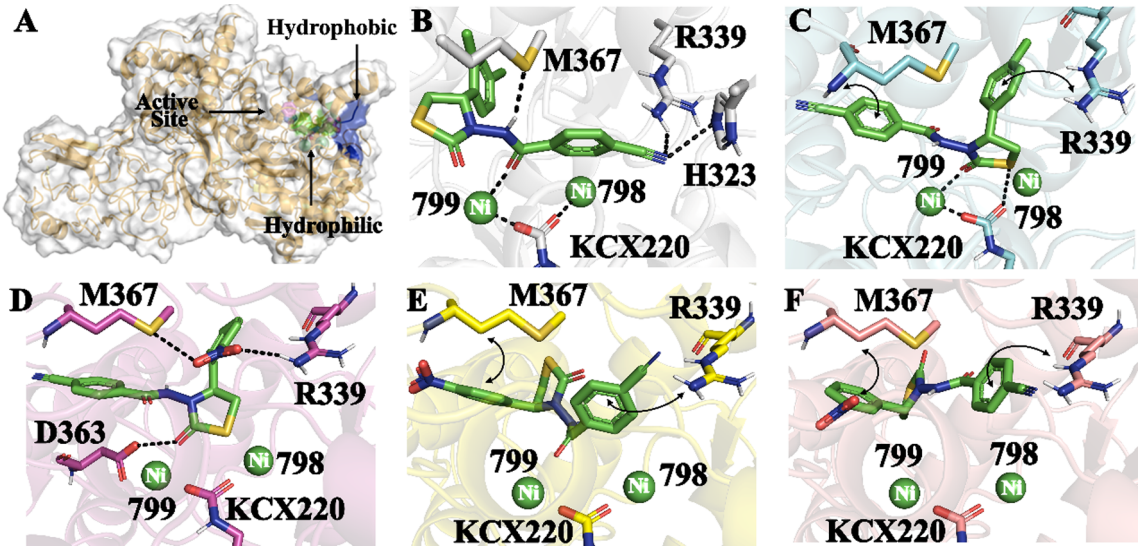

Fig. 3. The PL interaction profiles for most active compounds in the series against urease enzyme. **(A)** the hydrophobic (dark blue) and hydrophilic (dark green) region of urease enzyme, **(B)** the mode of interaction for highly potent compound **2k, (C)** for rank 2nd most active compound **2a**, (**D**) for rank 3rd active compound **2h (E)** for rank 4th active compound **2f** and (**F**) for rank 5th active compound **2e** among the series. Different ligands were colored dark green. Hydrogen bonding is shown in black color dotted lines, and the both sided arrows indicate the pi-stacking interaction.

the benzene ring to make π-π interaction to let sustain stabilization of the ring (Fig. 3c). In case of 3rd rank compound **2h** (**4.70 ± 0.03**) possess also EWG (NO_2 group) at *ortho* position over benzene ring, but showed less potency as compare with rank 1st and rank 2nd active compound, even though the magnitude of EWG effect for nitro group is much stronger than other halides but showed less potency. The high magnitude of EWG effect but showed less potency in comparison with other rank 1st and 2nd compound might be due to the PL interaction profile, and additionally might be due to the favorable interaction of both the Ni ions and KCX-220 in the case of rank 1st and 2nd, but not in case of this compound which carry nitro group as shown in Fig. 3d. The PL interaction profile for compound **2h** revealed less (i.e., R339, M367, and D363) as compare with PL interaction profile for most potent. Similar PL interaction profile was observed in case of rank 4th and 5th compounds **2f** (6.70 ± 0.05) and **2e** (8.30 ± 0.3), even though the IC_{50} values of both the compound seem different, the similarity in PL interaction profile (Fig. 3e and f) might be due to the same EWG, and differences possess in IC_{50} values might be different based on the

position, as we discussed in the beginning, that variation in position alter the enzyme activity.

More ever, the molecular docking results support well the experimental results based on the multiple interactions of ligands with key residues of the urease enzyme. From the current molecular docking results, it is evident that the quantity of the substituted groups and its position ultimately alter the enzyme activity. The most favorable activity was observed in case dual occupancy of substituted group.

3. Material and methods

All the reagents and chemicals were purchased from sigma Aldrich, USA. NMR experiments were performed on Avance Bruker AM 300 MHz machine. High Resolution Electron impact mass spectra (HREI-MS) were recorded on a Finnigan MAT-311A (Germany) mass spectrometer. Thin layer chromatography (TLC) was performed on precoated silica gel aluminum plates (Kieselgel 60254, E. Merck, Germany). Chromatograms were visualized by UV at 254 and 365 nm.

3.1. General route for the synthesis of arylhydrazide bearing Schiff bases/ thiazolidinone

We reacted and reflux hydrazine hydrate with 4-cyanobezoate to give aryl hydrazide as intermediate product (**I**). Synthesized intermediate (**I**) was used in two different ways. Firstly, intermediate (**I**) was reacted and refluxed with different substituted aldehydes/acetophenone to give arylhydrazide bearing Schiff bases product (**1a-r**). Secondly, intermediate (**I**) was reacted and refluxed with different substituted aldehydes to give hydrazide as second intermediate (**II**) which was then reacted and refluxed with thioglycolic acid to give arylhydrazide bearing thiazolidinone product (**2a-o**). The products were confirmed through ^{1}H, ^{13}C NMR and HR-EIMS analysis.

*3.1.1. N′-(4-chlorobenzylidene)-4-cyanobenzohydrazide (**1a**)*

^{1}H NMR (500 MHz, DMSO-d_6): δ12.0 (s, 1H, NH), 8.45 (s, CH), 7.96 (d, J = 6.55 Hz, 2H), 7.77 (d, J = 6.55 Hz, 2H), 7.63 (d, J = 6.6 Hz, 2H), 7.54 (d, J = 6.35 Hz, 2H); ^{13}C NMR (125 MHz, DMSO-d_6): δ 162.0, 146.7, 136.2, 134.5, 133.1, 132.2, 131.9, 129.5, 128.9, 128.8, 128.7, 128.5, 128.3, 128.3, 119; HR-EIMS calcd 283.05124 for $C_{15}H_{10}ClNO_3$ and was found 283.05112.

*3.1.2. 4-Cyano-N′-(3-hydroxy-4-methoxybenzylidene) benzohydrazide (**1b**)*

^{1}H NMR (500 MHz, DMSO-d_6): δ 11.75 (s, 1H, NH), 9.37 (br s, 1H, OH), 8.31 (s, CH), 7.94 (d, J = 6.1 Hz, 2H), 7.61 (d, J = 6.05 Hz, 2H), 7.29 (s, 1H), 7.07 (d, J = 6.65 Hz, 1H), 6.99 (d, J = 6.4 Hz, 1H), 3.87 (s, 3H, $-OCH_3$); ^{13}C NMR (125 MHz, DMSO-d_6): δ 161.78, 149.84, 148.28, 146.87, 136.38, 132.27, 129.44 (2C), 128.49 (2C), 127.03, 120.32, 112.32, 111.83, 55.54; HR-EIMS calcd 295.09569 for $C_{16}H_{13}N_3O_3$ found 295.09554.

*3.1.3. 4-Cyano-N′-(2-nitrobenzylidene) benzohydrazide (**1c**)*

^{1}H NMR (500 MHz, DMSO-d_6): δ 12.27 (s, 1H, NH), 8.89 (s, 1H, CH), 8.15 (dd, J = 6.25, 6.55 Hz, 2H), 7.99 (d, J = 6.55 Hz, 2H), 7.84 (t, J = 5.8 Hz, 1H), 7.71 (t, J = 6.1 Hz, 1H), 7.64 (d, J = 6.6 Hz, 2H); ^{13}C NMR (125 MHz, DMSO-d_6): δ 162.21, 148.20, 143.24, 136.84, 133.86 (2C), 131.65, 130.69, 129.63 (2C), 128.57 (2C), 127.92, 124.62 (2C); HR-EIMS calcd 294.07529 for $C_{15}H_{10}N_4O_3$ found 294.07513.

*3.1.4. 4-Cyano-N′-(4-(phenoxymethyl) benzylidene) benzohydrazide (**1d**)*

^{1}H NMR (500 MHz, DMSO-d_6): δ 11.82 (s, 1H, NH), 8.41 (s, 1H, CH), 7.96 (d, J = 6.85 Hz, 2H), 7.70 (d, J = 7.05 Hz, 2H), 7.61 (d, J = 6.95 Hz, 2H), 7.48 (d, J = 6.15 Hz, 2H), 7.42 (t, J = 6.15 Hz, 2H), 7.35 (t, J = 6.05 Hz, 1H), 7.12 (d, J = 7.1 Hz, 2H), 5.16 (s, 2H, CH_2); ^{13}C NMR (125 MHz, DMSO-d_6): δ 161.84, 159.97, 147.94, 136.70, 136.42, 132.24, 129.46 (2C), 128.72 (2C), 128.49 (2C), 128.41 (2C), 127.88 (2C), 127.71 (2C), 126.98, 115.15 (2C), 69.34; HR-EIMS calcd 355.13208 for $C_{22}H_{17}N_3O_2$ found 355.13181.

*3.1.5. 4-Cyano-N′-(4-hydroxybenzylidene) benzohydrazide (**1e**)*

^{1}H NMR (500 MHz, DMSO-d_6): δ 11.75 (s, 1H, NH), 9.98 (br s, 1H, OH), 8.36 (s, 1H, CH), 7.95 (d, J = 6.85 Hz, 2H), 7.61 (q, 4H), 6.86 (d, J = 6.9 Hz, 2H); ^{13}C NMR (125 MHz, DMSO-d_6): δ 161.73, 159.53, 148.46, 136.35, 132.31 (2C), 129.42 (2C), 128.88 (2C), 128.47 (2C), 125.13, 115.70 (2C); HR-EIMS calcd 265.08513 for $C_{15}H_{11}N_3O_2$ found 265.08499.

*3.1.6. 4-Cyano-N′-(2,4-dichlorobenzylidene) benzohydrazide (**1f**)*

^{1}H NMR (500 MHz, DMSO-d_6): δ 12.19 (s, 1H, NH), 8.81 (s, 1H, CH), 8.04 (d, J = 7.1 Hz, 2H), 7.97 (d, J = 6.9 Hz, 2H), 7.73 (s, 1H), 7.64 (d, J = 6.95 Hz, 1H), 7.54 (d, J = 6.4 Hz, 1H); ^{13}C NMR (125 MHz, DMSO-d_6): δ 162.08, 142.88, 136.81, 135.15, 133.88, 131.71, 130.59, 129.57 (2C), 129.36 (2C), 128.61 (2C), 128.06, 128.03; HR-EIMS calcd 317.01227 for $C_{15}H_9N_3O$ found 317.01216.

*3.1.7. N′-(anthracen-9-ylmethylene)-4-cyanobenzohydrazide (**1g**)*

^{1}H NMR (500 MHz, DMSO-d_6): δ 12.18 (s, 1H, NH), 9.67 (s, 1H, CH), 8.76 (d, J = 6.05 Hz, 4H), 8.20 (t, J = 8.75 Hz, 2H), 8.07 (d, J = 6.5 Hz, 2H), 7.91 (d, J = 7.05 Hz, 1H), 7.69 (m, 2H), 7.61 (m, 2H); ^{13}C NMR (125 MHz, DMSO-d_6): δ 161.97, 147.34, 136.70, 130.97, 130.89, 129.72, 129.61 (2C), 129.56 (2C), 129.03 (2C), 129.00 (2C), 128.68 (2C), 127.96, 127.21, 126.87, 125.56, 124.96, 124.82, 124.77; HR-EIMS calcd 349.12151 for $C_{23}H_{15}N_3O$ found 349.12149.

*3.1.8. 4-Cyano-N′-(4-(dimethylamino) benzylidene) benzohydrazide (**1h**)*

^{1}H NMR (500 MHz, DMSO-d_6): δ 11.64 (s, 1H, NH), 8.32 (s, 1H, CH), 7.94 (d, J = 6.9 Hz, 2H), 7.60 (dd, J = 6.95, 7.15 Hz, 4H), 6.76 (d, J = 7.15 Hz, 2H), 2.97(s, 6H, $N(CH_3)_2$); ^{13}C NMR (125 MHz, DMSO-d_6): δ 161.55, 151.53, 148.96, 136.22, 132.47, 129.37, 128.46 (4C), 128.44 (2C), 121.44, 111.74 (2C), 45.6 (2C); HR-EIMS calcd 292.13241 for $C_{17}H_{16}N_4O$ found HR-EIMS calcd 292.13240.

*3.1.9. N′-(5-bromo-2-methoxybenzylidene)-4-cyanobenzohydrazide (**1i**)*

^{1}H NMR (500 MHz, DMSO-d_6): δ 12.03 (s, 1H, NH), 8.37 (s, 1H, CH), 7.98 (t, J = 6.7 Hz, 3H), 7.61 (dd, J = 6.7, 6.25 Hz, 4H), 7.10 (d, J = 7.25 Hz, 1H), 3.87 (s, 3H, OCH_3); ^{13}C NMR (125 MHz, DMSO-d_6): δ 161.91, 156.85, 141.80, 136.66, 133.63, 131.80, 129.51, 128.52 (2C), 127.41 (2C), 124.40, 114.35 (2C), 112.46, 56.18; HR-EIMS calcd 357.01129 for $C_{16}H_{12}BrN_3O_2$ found 357.01121.

*3.1.10. 4-Cyano-N′-(3,4-dihydroxybenzylidene) benzohydrazide (**1j**)*

^{1}H NMR (500 MHz, DMSO-d_6): δ 11.68 (s, 1H, NH), 9.39 (s, 2H, OH), 8.27 (s, 1H, CH), 7.94 (d, J = 6.35 Hz, 2H), 7.82 (d, J = 5.25 Hz, 2H), 7.61 (dd, J = 6.8, 2.6 Hz, 1H), 7.27 (s, 1H), 6.96 (d, J = 6.3 Hz, 1H), 6.81 (d, J = 6.6 Hz, 1H); ^{13}C NMR (125 MHz, DMSO-d_6): δ 161.72, 148.66, 148.05, 145.70, 136.33, 132.32, 129.41 (2C), 128.47 (2C), 125.62, 120.65 (2C), 115.54, 112.71; HR-EIMS calcd 211.08004 for $C_{15}H_{11}N_3O_3$ found 211.07991.

*3.1.11. N′-(3-aminobenzylidene)-4-cyanobenzohydrazide (**1k**)*

^{1}H NMR (500 MHz, DMSO-d_6): δ 11.79 (s, 1H, NH), 8.29 (s, 1H, CH), 7.94 (d, J = 6.5 Hz, 2H), 7.61 (d, J = 6.4 Hz, 2H), 7.10 (t, J = 6.25 Hz, 1H), 7.00 (s, 1H), 6.81 (d, J = 5.75 Hz, 1H), 6.64 (d, J = 5.9 Hz, 1H), 5.27 (s, 2H, NH_2); ^{13}C NMR (125 MHz, DMSO-d_6): δ 161.86, 149.01, 148.94, 148.92, 136.43, 134.64, 132.21, 129.56, 129.48, 129.20, 128.51, 116.08, 115.78, 115.72, 111.19; HR-EIMS calcd 264.10111 for $C_{15}H_{12}N_4O$ found 264.10102.

*3.1.12. 4-Cyano-N′-(4-nitrobenzylidene) benzohydrazide (**1l**)*

^{1}H NMR (500 MHz, DMSO-d_6): δ 11.06 (s, 1H, NH), 8.27 (s, 1H, CH), 8.10 (d, J = 6.1 Hz, 2H), 7.9 (d, J = 6.1 Hz, 2H), 7.77 (d, J = 6.5 Hz, 2H), 7.67 (d, J = 6.5 Hz, 2H); ^{13}C NMR (125 MHz, DMSO-

d_6): δ 161.10, 152.48, 147.61, 144.13, 136.49, 132.58 (2C), 130.22, 129.95 (2C), 128.49 (2C), 127.61 (2C), 123.53; HR-EIMS calcd 294.05729 for $C_{15}H_{10}N_4O_3$ found 294.05717.

*3.1.13. 4-Cyano-N′-(1,3-diphenylpropylidene) benzohydrazide (**1m**)*

^{1}H NMR (500 MHz, DMSO-d_6): δ 12.27 (s, 1H, NH), 7.91 (d, J = 5.35 Hz, 4H), 7.72 (d, J = 5.8 Hz, 2H), 7.62 (d, J = 6.5 Hz, 2H), 7.54 (m, 5H), 7.36 (t, J = 5.1 Hz, 1H), 2.08 (d, J = 5.6 Hz, 2H), 1.99 (s, 2H); ^{13}C NMR (125 MHz, DMSO-d_6): δ 186.13, 164.71, 164.65, 155.04, 143.80, 139.01, 136.83, 130.98, 130.88, 129.60, 129.57, 129.52, 129.43, 128.76, 128.72, 128.65, 128.34, 127.96, 127.73, 126.84, 124.56, 92.93, 91.51; HR-EIMS calcd 353.15281 for $C_{23}H_{19}N_3O$ found 353.15270.

*3.1.14. 4-Cyano-N′-(naphthalen-2-ylmethylene) benzohydrazide (**1n**)*

^{1}H NMR (500 MHz, DMSO-d_6): δ 11.86 (s, 1H, NH), 10.78 (s, 1H, OH), 8.33 (s, 1H, CH), 7.95 (d, J = 6.1 Hz, 2H), 7.73 (s, 1H), 7.61 (d, J = 6 Hz, 2H), 7.55 (d, J = 6.75 Hz, 1H), 7.06 (d, J = 6.65 Hz, 1H); ^{13}C NMR (125 MHz, DMSO-d_6): δ 161.90, 154.92, 146.92, 136.46, 132.13, 129.47, 128.49 (2C), 128.37 (2C), 127.25, 126.46, 120.31, 116.85 (2C); HR-EIMS calcd 299.04615 for $C_{15}H_{10}ClN_3O_2$ found 299.04601.

*3.1.15. N′-(3-chloro-4-hydroxybenzylidene)-4-cyanobenzohydrazide (**1o**)*

^{1}H NMR (500 MHz, DMSO-d_6): δ 12.15 (s, 1H, NH), 8.64 (s, 1H, CH), 8.16 (s, 1H), 8.02 (m, 6H), 7.63 (d, J = 6.95 Hz, 2H), 7.58 (q, 2H); ^{13}C NMR (125 MHz, DMSO-d_6): δ 162.13, 148.04, 136.52, 133.73, 132.83, 132.18, 132.02, 129.59 (2C), 128.75, 128.53, 128.47, 128.30 (2C), 127.74, 127.11, 126.72, 122.66; HR-EIMS calcd 299.10586 for $C_{19}H_{13}N_3O$ found 299.10575.

*3.1.16. 4-Cyano-N′-((1-hydroxynaphthalen-2-yl) methylene) benzohydrazide (**1p**)*

^{1}H NMR (500 MHz, DMSO-d_6): δ 12.56 (s, 1H, OH), 9.49 (s, 1H, NH), 8.26 (s, 1H, CH), 8.03 (d, J = 6.8 Hz, 2H), 7.95 (dd, J = 7.4, 6.6 Hz, 3H), 7.68 (d, J = 6.85 Hz, 2H), 7.63 (t, J = 6.05 Hz, 1H), 7.43 (t, J = 6 Hz, 1H), 7.25 (d, J = 7.35 Hz, 1H); ^{13}C NMR (125 MHz, DMSO-d_6): δ 161.46, 158.15, 147.07, 136.87, 132.81, 132.60, 131.40, 129.46 (2C), 128.94, 128.71, 128.47 (2C), 127.75 (2C), 123.49, 120.63, 118.90, 108.47; HR-EIMS calcd 315.1007 for $C_{19}H_{13}N_3O_2$ found 315.0994.

*3.1.17. 4-Cyano-N′-(4-hydroxy-3,5-dimethylbenzylidene) benzohydrazide (**1q**)*

^{1}H NMR (500 MHz, DMSO-d_6): δ 11.72 (s, 1H, NH), 8.40 (s, 1H, CH), 7.94 (d, J = 6.9 Hz, 2H), 7.61 (d, J = 6.9 Hz, 2H), 7.52 (d, J = 7.45 Hz, 2H), 1.3 (s, 6H, CH_3). ^{13}C NMR (125 MHz, DMSO-d_6): δ 161.74, 156.20, 149.68 (2C), 139.16, 136.34, 132.33, 129.40 (2C), 128.49 (2C), 125.46 (2C), 123.91 (2C), 30.12 (2C); HR-EIMS calcd 293.1164 for $C_{17}H_{15}N_3O_2$ found 293.1153.

*3.1.18. 4-Cyano-N′-(4-hydroxy-3-methoxybenzylidene) benzohydrazide (**1r**)*

^{1}H NMR (500 MHz, DMSO-d_6): δ 11.75 (s, 1H, NH), 9.61 (s, 1H, OH), 8.34 (s, 1H, CH), 7.94 (d, J = 6.85 Hz, 2H), 7.61 (d, J = 6.9 Hz, 2H), 7.32 (s, 1H), 7.10 (d, J = 6.6 Hz, 1H), 6.86 (d, J = 6.65 Hz, 1H), 3.8 (s, 3H, OCH_3); ^{13}C NMR (125 MHz, DMSO-d_6): δ 161.77, 149.09, 148.67, 148.02, 136.35, 132.31 (2C), 129.43 (2C), 128.49 (2C), 125.56, 122.20, 115.42, 108.99, 55.54; HR-EIMS calcd 295.09569 for $C_{16}H_{13}N_3O_3$ found 295.09558.

*3.1.19. N-(2-(4-chlorophenyl)-4-oxothiazolidin-3-yl)-4-cyanobenzamide (**2a**)*

^{1}H NMR (500 MHz, DMSO-d_6): δ 11.99 (s, NH, 1H), 8.45 (d, J = 7.7 Hz, 2H), 8.24 (d, J = 7.7 Hz, 2H), 7.56 (d, J = 6.6 Hz, 2H), 8.17 (d, J = 6.5 Hz, 2H), 6.01 (s, S-CH, 1H), 3.60 (s, S-CH_2, 2H); ^{13}C NMR (125 MHz, DMSO-d_6): δ 171.7, 168.6, 140.4, 139.8, 134.9, 134.8, 134.8, 134.2, 131.5, 131.5, 130.6, 130.6, 130.2, 130.2, 120.4, 117.8, 67.6, 37.3; HR-EIMS calcd 357.0338 for $C_{17}H_{12}ClN_3O_2S$ found 357.0324.

3.1.20. N-(4-(3-bromo-5-methoxyphenyl)-2-oxothiazolidin-3-yl)-4-cyanobenzamide (2b)

^{1}H NMR (500 MHz, DMSO-d_6): δ 11.7 (s, NH, 1H), 8.39 (d, J = 7.1 Hz, 2H), 8.0 (d, J = 7.05 Hz, 2H), 7.33 (d, J = 1.3 Hz, 1H), 7.33 (d, J = 1.3 Hz, 1H), 7.01 (s, 1H), 5.90 (s, S-CH, 1H), 3.89 (s, −OCH_3, 3H), 3.76 (s, S-CH_2, 2H). ^{13}C NMR (125 MHz, DMSO-d_6): δ 171.7, 168.6, 161.4, 149.1, 137.8, 134.7, 134.7, 130.9, 130.9, 126.2, 125.8, 120.8, 119.9, 117.6, 112.9, 65.2, 54.8, 34.6; HR-EIMS calcd 430.9939 for $C_{18}H_{14}BrN_3O_3S$ found 430.9925.

*3.1.21. 4-Cyano-N-(4-oxo-2-(4-phenoxy-methyl) phenyl) thiazolidine-3-yl) benzamide (**2c**)*

^{1}H NMR (500 MHz, DMSO-d_6): δ 11.8 (s, NH, 1H), 8.23 (d, J = 7.3 Hz, 2H), 7.98 (d, J = 7.3 Hz, 2H), 7.65 (m 4H), 7.34 (m, 4H), 6.91 (m, 1H), 5.89 (s, S-CH, 1H), 5.56 (s, −OCH_2, 2H), 3.67 (s, S-CH_2, 2H); ^{13}C NMR (125 MHz, DMSO-d_6): δ 171.1, 168.4, 161.1, 145.3, 137.5, 135.9, 134.1 (2C), 130.3 (2C), 129.1 (2C), 126.2 (2C), 125.8 (2C), 123.3, 120.3, 117.4, 115.7 (2C), 65.2, 34.6; HR-EIMS calcd 429.1147 for $C_{24}H_{19}N_3O_3S$ found 429.1136.

*3.1.22. N-(2-(anthracen-9-yl)-4-oxothiazolidin-3-yl)-4-cyanobenzamide (**2d**)*

^{1}H NMR (500 MHz, DMSO-d_6): δ 10.09 (s, NH, 1H), 8.51 (d, J = 7.3 Hz, 2H), 8.37 (d, J = 7.3 Hz, 2H), 8.19 (s, 1H), 7.99 (d, J = 6.9 Hz, 2H), 7.97 (d, J = 6.5 Hz, 2H), 7.78 (m, 4H), 6.12 (s, S-CH, 1H), 3.75 (s, S-CH_2, 2H); ^{13}C NMR (125 MHz, DMSO-d_6): δ 171.1, 168.4, 137.8, 134.5 (3C), 133.4 (2C), 131.2 (2C), 129.8 (2C), 128.6 (2C), 127.5 (2C), 126.8 (2C), 126.3 (2C), 125.6, 120.3, 117.5, 64.1, 34.6; HR-EIMS calcd 423.1041 for $C_{25}H_{17}N_3O_2S$ found 423.1030.

*3.1.23. 4-Cyano-N-(2-(3-nitrophenyl)-4-oxothiazolidin-3-yl) benzamide (**2e**)*

^{1}H NMR (500 MHz, DMSO-d_6): δ 11.51 (s, NH, 1H), 8.51 (d, J = 1.1 Hz, 1H), 8.43 (d, J = 7.3 Hz, 2H), 8.35 (d, J = 7.3 Hz, 3H), 7.85 (d, J = 6.3 Hz, 1H), 7.69 (t, J = 6.3 Hz, 1H), 6.01 (s, S-CH, 1H), 3.78 (s, S-CH_2, 2H); ^{13}C NMR (125 MHz, DMSO-d_6): δ 171.1, 168.4, 148.3, 142.5, 137.8, 134.9, 133.6 (2C), 130.1, 129.7, 129.7, 127.1, 124.5, 120.3, 117.6, 65.6, 34.6; HR-EIMS calcd 368.0579 for $C_{17}H_{12}N_4O_4S$ found 368.0564.

*3.1.24. 4-Cyano-N-(2-(4-nitrophenyl)-4-oxothiazolidin-3-ylbenzamide (**2f**)*

^{1}H NMR (500 MHz, DMSO-d_6): δ 11.51 (s, NH, 1H), 8.51 (d, J = 7.4 Hz, 2H), 8.39 (d, J = 7.3 Hz, 2H), 8.13 (d, J = 7.3 Hz, 2H), 7.82 (d, J = 7.4 Hz, 2H), 6.10 (s, S-CH, 1H), 3.90 (s, S-CH_2, 2H); ^{13}C NMR (125 MHz, DMSO-d_6): δ 171.1, 168.4, 148.3, 147.8, 137.8, 134.6 (2C), 131.1 (2C), 129.4 (2C), 125.2 (2C), 120.3, 117.6, 66.2, 36.4; HR-EIMS calcd 368.0579 for $C_{17}H_{12}N_4O_4S$ found 368.0564.

*3.1.25. 4-Cyano-N-(2-(2-hydroxynapthalen-1-yl)-4-oxothiazolidin-3-yl) benzamide (**2g**)*

^{1}H NMR (500 MHz, DMSO-d_6): δ 11.78 (s, NH, 1H), 10.11 (br s, OH, 1H), 8.39 (d, J = 7.3 Hz, 2H), 8.27 (d, J = 7.3 Hz, 2H), 8.09 (d, J = 6.8 Hz, 1H), 7.91 (m, 2H), 7.54 (m, 2H), 7.13 (d, J = 6.4 Hz, 1H), 5.99 (s, S-CH, 1H), 3.78 (s, S-CH_2, 2H); ^{13}C NMR (125 MHz, DMSO-d_6): δ 182.3, 171.1, 168.4, 152.4, 137.8, 135.6, 135.2, 133.8 (2C), 130.7 (2C), 127.9 (2C), 120.3, 120.1 (2C), 117.3, 96.7, 88.5, 64.4, 33.2; HR-EIMS calcd 389.0834 for $C_{21}H_{15}N_3O_3S$ found 389.0822.

*3.1.26. 4-Cyano-N-(2-(2-nitrophenyl)-4-oxothiazolidin-3-yl) benzamide (**2h**)*

^{1}H NMR (500 MHz, DMSO-d_6): δ 11.62 (s, NH, 1H), 8.43 (d,

J = 7.3 Hz, 2H), 8.28 (d, J = 7.3 Hz, 2H), 8.02 (d, J = 6.3 Hz, 1H), 7.69 (m, 2H), 7.31 (d, J = 6.5 Hz, 1H), 6.12 (s, S-CH, 1H), 3.81 (s, S-CH_2, 2H); ^{13}C NMR (125 MHz, DMSO-d_6): δ 170.3, 167.6, 150.1, 138.5, 135.3, 134.7, 133.1 (2C), 130.6, 129.7, 129.1 (2C), 128.7, 125.6, 119.8, 116.9, 63.8, 36.2; HR-EIMS calcd 368.0579 for $C_{17}H_{12}N_4O_4S$ found 368.0565.

3.1.27. 4-Cyano-N-(2-(2,3-dimethylphenyl)-4-oxothiazolidin-3-yl) benzamide (2i)

^{1}H NMR (500 MHz, DMSO-d_6): δ 11.45 (s, NH, 1H), 8.39 (d, J = 7.3 Hz, 2H), 8.27 (d, J = 7.3 Hz, 2H), 7.61 (d, J = 6.7 Hz, 1H), 7.43 (m, 1H), 7.28 (d, J = 6.7 Hz, 1H), 5.99 (s, S-CH, 1H), 3.76 (s, S-CH_2, 2H), 2.43 (s, $-CH_3$, 3H), 2.39 (s, $-CH_3$, 3H); ^{13}C NMR (125 MHz, DMSO-d_6): δ 171.1, 168.1, 140.4, 137.1, 136.8, 136.3, 133.4 (2C), 130.8, 130.2 (2C), 126.9, 126.6, 120.1, 117.2, 67.4, 37.1, 22.9, 19.4; HR-EIMS calcd 351.1041 for $C_{19}H_{17}N_3O_2S$ found 351.1026.

3.1.28. 4-Cyano-N-(2-(2-hydroxyphenyl)-4-oxothiazolidin-3-yl) benzamide (2j)

^{1}H NMR (500 MHz, DMSO-d_6): δ 11.52 (s, NH, 1H), 10.02 (br s, OH, 1H), 8.45 (d, J = 7.3 Hz, 2H), 8.34 (d, J = 7.3 Hz, 2H), 7.19 (m, 2H), 6.83 (m, 2H), 6.12 (s, S-CH, 1H), 3.81 (s, S-CH_2, 2H); ^{13}C NMR (125 MHz, DMSO-d_6): δ 169.9, 167.5, 154.6, 137.5, 132.9 (2C), 130.9, 130.6 (2C), 130.2, 122.9, 120.3, 120.1, 117.5, 116.7, 63.8, 36.5; HR-EIMS calcd 339.0677 for $C_{17}H_{13}N_3O_3S$ found 339.0668.

3.1.29. 4-Cyano-N-(2-(2-hydroxyphenyl)-4-oxothiazolidin-3-yl) benzamide (2k)

^{1}H NMR (500 MHz, DMSO-d_6): δ 11.46 (s, NH, 1H), 8.37 (d, J = 7.3 Hz, 2H), 8.24 (d, J = 7.3 Hz, 2H), 7.85 (d, J = 1.3 Hz, 1H), 7.34 (d, J = 6.7 Hz, 1H), 7.21 (d, J = 6.7 Hz, 1H), 6.02 (s, S-CH, 1H), 3.77 (s, S-CH_2, 2H); ^{13}C NMR (125 MHz, DMSO-d_6): δ 170.3, 168.1, 138.5, 136.7, 135.6, 133.7 (2C), 132.3, 131.8, 130.5 (2C), 126.7, 119.8, 117.8, 102.2, 64.5, 36.2; HR-EIMS calcd 390.9949 for $C_{17}H_{11}Cl_2N_3O_2S$ found 390.9936.

3.1.30. 4-Cyano-N-(2-(3-methoxy-4-(phenoxymethyl)phenyl)-4-oxothiazolidin-3-yl) benzamide (2l)

^{1}H NMR (500 MHz, DMSO-d_6): δ 11.52 (s, NH, 1H), 8.45 (d, J = 7.3 Hz, 2H), 8.31 (d, J = 7.3 Hz, 2H), 7.56 (m, 3H), 7.21 (m, 3H), 6.89 (m, 2H), 5.99 (s, S-CH, 1H), 5.34 (s, $-OCH_2$, 2H), 3.89 (s, $-OCH_3$, 3H), 3.78 (s, S-CH_2, 2H); ^{13}C NMR (125 MHz, DMSO-d_6): δ 171.1, 167.4, 161.4, 157.8, 141.0, 137.4, 133.2 (2C), 131.5 (2C), 130.7 (2C), 130.4, 126.2, 122.7, 122.3, 120.1, 116.9, 115.7 (2C), 114.4, 66.5, 64.5, 57.8, 37.1; HR-EIMS calcd 459.1252 for $C_{25}H_{21}N_3O_4S$ found 459.1238.

3.1.31. 4-Cyano-N-(2-(naphthalen-2-yl)-4-oxothiazolidin-3-yl) benzamide (2m)

^{1}H NMR (500 MHz, DMSO-d_6): δ 11.63 (s, NH, 1H), 8.23 (d, J = 7.3 Hz, 2H), 8.16 (d, J = 7.3 Hz, 2H), 7.86 (m, 3H), 7.43 (m, 3H), 7.21 (d, J = 6.5 Hz, 1H), 6.02 (s, S-CH, 1H), 3.68 (s, S-CH_2, 2H); ^{13}C NMR (125 MHz, DMSO-d_6): δ 170.5, 169.1, 137.6, 136.7, 135.3, 133.6 (2C), 132.9, 131.3 (2C), 130.9, 129.4, 129.1, 128.9, 128.7, 127.8, 126.9, 119.8, 117.1, 68.1, 36.8; HR-EIMS calcd 373.0885 for $C_{21}H_{15}N_3O_2S$ found 373.0874.

3.1.32. 4-Cyano-N-(2-(2,4-dimethylphenyl)-4-oxothiazolidin-3-yl) benzamide (2n)

^{1}H NMR (500 MHz, DMSO-d_6): δ 11.67 (s, NH, 1H), 8.33 (d, J = 7.3 Hz, 2H), 8.21 (d, J = 7.3 Hz, 2H), 7.25 (m, 2H), 6.90 (m, 1H), 5.99 (s, S-CH, 1H), 3.76 (s, S-CH_2, 2H), 2.54 (s, $-CH_3$, 3H), 2.42 (s, $-CH_3$, 3H); ^{13}C NMR (125 MHz, DMSO-d_6): δ 171.3, 168.0, 152.2, 138.6, 137.7, 137.3, 133.5 (2C), 131.2, 130.4, 130.1 (2C), 126.8, 120.1, 117.8, 67.4, 37.3, 24.5, 20.9; HR-EIMS calcd 351.1041 for $C_{19}H_{17}N_3O_2S$ found 351.1029.

3.1.33. N-(2-(2-bromo-4-methoxyphenyl)-4-oxothiazolidin-3-yl)-4-cyanobenzamide (2o)

^{1}H NMR (500 MHz, DMSO-d_6): δ 11.59 (s, NH, 1H), 8.48 (d, J = 7.3 Hz, 2H), 8.31 (d, J = 7.3 Hz, 2H), 7.54 (s, 1H), 7.27 (d, J = 6.4 Hz, 1H), 6.99 (d, J = 6.4 Hz, 1H), 6.13 (s, S-CH, 1H), 3.98 (s, $-CH_3$, 3H), 3.76 (s, S-CH_2, 2H); ^{13}C NMR (125 MHz, DMSO-d_6): δ 170.1, 167.7, 159.8, 137.7, 135.6, 133.3 (2C), 132.5, 130.6 (2C), 125.8, 120.2, 118.5, 117.6, 115.1, 65.2, 57.8, 36.8; HR-EIMS calcd 430.9939 for $C_{18}H_{14}BrN_3O_3S$ found 430.9928.

3.2. Molecular docking protocol for α-amylase

Docking simulation was performed targeting the crystal structure of amylase (PDB ID: 4W93) [34] in order to reveal the binding modes of synthesized arylhydrazide bearing Schiff base derivatives (**1a-r**), For the purpose of docking studies, the crystal structure of the amylase was optimized using protein preparation module in Discovery Studio 2018 (Dassault Systems BIOVIA, USA) [35]. The crystal structure was retrieved from the protein data bank (PDB) and further, the structure was optimized by removing the water molecules, hetero atoms, and co-factors. Hydrogen bonds, missing atoms, and charges were computed. The synthesized arylhydrazide bearing Schiff base derivatives (**1a-r**) used in these docking studies was prepared and optimized using built and Ligand Preparation module implemented in Discovery Studio 2018 (Dassault Systemes BIOVIA, USA). For the purpose of docking; Gold docking tool was used, Ligand preparation includes generating various tautomer's, assigning bond orders and stereochemistry. Additionally, receptor grid was generated around the amylase active site by choosing centroid of complexed ligand (Montbretin A). The active site was defined with a radius of 12 Å around the Montbretin A binding site. Docking calculations were accomplished using Chem PLP scoring function [36]. The docking results were further analyzed, and each derivative binding mode was visually inspected using Discover studio visualizer.

3.3. Molecular docking protocol for urease

Molecular Operating Environment (MOE) modeling package [37] was utilized for molecular docking study, in order to explore the binding mode of the synthesized compounds within the active site of urease enzyme. First, the 3D structures for all the synthesized compounds were generated using implemented builder module in MOE. Next, all the generated 3D structures of all the compounds were protonated and energy minimized using the default parameters of the MOE (gradient: 0.05, Force Field: MMFF94X). Now the crystal structure of urease enzyme was retrieved from online free database, the protein databank (PDB ID 4ubp). The crystal structure was subjected to MOE in order to conduct the preparation step, all the water molecules has been removed, and further protonation was done using default parameters of structure preparation module implemented in MOE. Next the protonated crystal structure were subjected to energy minimization step to get a stable conformation. Finally, refined crystal structure was used for further docking study using the default parameters of MOE, i.e., Placement: Triangle Matcher, rescoring 1: London dG, Refinement: Force field, Rescoring 2: GBVI/WSA. Before running the docking protocol, for ligand, total ten conformations were selected. The top-ranked conformations by docking score were selected for protein-ligand interaction (PL) analysis.

3.4. Urease inhibitory assay

Spectrophotometrically urease inhibition assay was performed. For urease inhibition assay 5 μL of synthetic compound was incubated with 25 μL of urease solution (1 U/well) (250 μL) at 30 °C for 15 min. After that, 55 μL substrate urea with 100 mM concentration was added and the plate was again incubated at 30 °C. After incubation 70 μL of basic

Table 2
α-Amylase inhibitory potential of arylhydrazide bearing Schiff bases.

S. NO	IC_{50} value	S. NO	IC_{50} value
1a	2.10 ± 0.10	**1j**	0.80 ± 0.05
1b	1.20 ± 0.10	**1k**	1.00 ± 0.05
1c	1.70 ± 0.10	**1l**	1.90 ± 0.10
1d	3.40 ± 0.20	**1m**	9.40 ± 0.30
1e	1.10 ± 0.10	**1n**	1.40 ± 1.0
1f	1.30 ± 0.10	**1o**	2.20 ± 0.10
1g	12.30 ± 0.50	**1p**	1.90 ± 0.10
1h	2.10 ± 0.10	**1q**	2.10 ± 0.20
1i	4.30 ± 0.20	**1r**	0.90 ± 0.05
Acarbose			1.70 ± 0.10 μM

± = Standard error mean.

Table 3
Urease inhibitory potential of arylhydrazide bearing thiazolidinone.

S. No	IC_{50} value (μM)	S. No	IC_{50} value (μM)
2a	4.60 ± 0.02	**2i**	22.20 ± 0.60
2b	16.90 ± 0.8	**2j**	5.40 ± 0.02
2c	22.20 ± 0.70	**2k**	4.10 ± 0.02
2d	27.2 ± 0.80	**2l**	19.80 ± 0.60
2e	8.30 ± 0.3	**2m**	24.2 ± 0.80
2f	6.70 ± 0.05	**2n**	28.20 ± 0.60
2g	11.20 ± 0.04	**2o**	38.20 ± 1.10
2h	4.70 ± 0.03	**Thiourea**	21.40 ± 0.21

± = Standard error mean.

reagent (0.5% w/v NaOH and 0.1% NaOCl) and 45 μL of carbolic acid (1% w/v carbolic acid and 0.005% w/v Na_2[Fe(CN)5NO]) were added at each well. Again, plate was incubated for 50 min at 30 °C. Rate of production ammonia was used for determining urease inhibitory activity by following Weather burn method and change in absorbance was monitored at 630 nm on a ELISA plate reader (Spectra Max M2, Molecular Devices, CA, USA) [38]. Thiourea was used as a standard compound [39]. All assays were performed in triplicate.

3.5. α-amylase inhibition assay

The α-amylase inhibition was determined by an assay modified from Kwon, Apostolidis & Shetty [40,41]. A total of 40 μL of sample and 40 μL of 0.02 M sodium phosphate buffer (pH 6.9 with 0.006 M sodium chloride) containing α- amylase solution (Porcine pancreatic α- amylase) (0.5 mg/ml) were incubated at 25 °C for 10 min. After pre-incubation, 40 μL of a 1% starch solution in 0.02 M sodium phosphate buffer (pH 6.9 with 0.006 M sodium chloride) was added to each tube at 5 s intervals. The reaction mixtures were then incubated at 25 °C for 10 min. The reaction was stopped with 100 μL of dinitrosalicylic acid colour reagent. The test tubes were then incubated in a boiling water bath for 5 min and cooled to room temperature. The reaction mixture was then diluted after adding 900 μL distilled water and the absorbance was measured at 540 nm. Acarbose was used as a standard drug. All assays were performed in triplicate.

Calculation of the concentration of compound required to scavenge 50% of the radical (IC_{50}) as per formula below:

$$I\% = (Ac - As)/Ac \times 100$$

Ac = the absorbance of the control
As = the absorbance of the sample.

4. Conclusion

Thirty-three analogs of arylhydrazide bearing Schiff bases/thiazolidinone (**1–33**) were synthesized and characterized through ^1H, ^{13}C NMR and HR-EIMS techniques. Analogs **1a-r** was evaluated against α-amylase inhibitory potential and exhibited varied degree of activity ranging between 0.8 ± 0.05 and 12.50 ± 0.5 μM (Table 2). Among the synthesized analogs, six analogs showed an excellent inhibitory potential as compare to the standard acarbose while all other analogs showed good to moderate activity. Analogs **2a-o** was evaluated against urease inhibitory potential showed IC_{50} value ranging between 4.10 ± 0.02–38.20 ± 1.10 μM (Table 3). Among the synthesized analogs, nine analogs showed an excellent inhibitory potential as compare to the standard thiourea while all other analogs showed good to moderate activity. SAR of analogs was established and was confirmed through molecular docking studies.

Acknowledgement

Authors would like to acknowledge Higher Education Commission of Pakistan for providing a research grant under National Research Program for Universities under project No. 5721 & 5092.

References

[1] F. Payan, Biochim. Biophys. Acta 1697 (2004) 171–180.
[2] E.A. Al Sherif, Flora 204 (2008) 737–746.
[3] B. Odhav, K. Thangaraj, K. Nonhlanhla, B. Himansu, J. Med. Plants Res. 4 (2010) 1502–1507.
[4] A. Fred-Jaiyesimi, A. Kio, W. Richard, Food Chem. 116 (2009) 285–288.
[5] R.P. Logan, M.M. Walker, Bacteriol. Med. J. 323 (2001) 920–922.
[6] B. Bano, K.M. Khan, A. Lodhi, U. Salar, F. Begum, M. Ali, M. Taha, S. Perveen, Bioorg. Chem. 80 (2018) 129–144.
[7] A.R.S. Hassani, N. Ordouzadeh, A. Ghaemi, N. Amirmozafari, K. Hamdi, R. Nazari, Indian J. Med. Microbiol. 27 (2009) 30–34.
[8] P. Giocchini, A. Nastri, C. Marzadori, L.V. Antisari, C. Gessa, Biol. Fert. Soils 36 (2002) 129–135.
[9] M.F. Mahomoodally, G. Zengin, D.Z. Dimitrova, A. Mollica, A. Stefanucci, K.I. Sinan, M.Z. Aumeeruddy, Ind. Crops Prod. 133 (2019) 373–382.
[10] M.F. Mahomoodally, A. Mollica, A. Stefanucci, M.Z. Aumeeruddy, R. Poorneeka, G. Zengin, Ind. Crops Prod. 126 (2018) 13–21.
[11] A. Mollica, G. Zengin, M. Locatelli, A. Stefanucci, G. Macedonio, G. Bellagamba, O. Onaolapo, A. Onaolapo, F. Azeez, A. Ayileka, E. Novellino, Food Chem. Toxicol. (2017) 1–11.
[12] F. Trampetti, C. Pereira, M.J. Rodrigues, O. Celaj, B.D. Abrosca, G. Zengin, A. Mollica, A. Stefanucci, L. Custodio, Comput. Biol. Chem. 165 (2019) 119–128.
[13] A. Uysal, O.Y. Ozer, G. Zengin, A. Stefanucci, A. Mollica, C.M.N.P. Allain, M.F. Mahomoodally, Comput. Biol. Chem. 78 (2019) 64–73.
[14] G. Zengin, M. Locatelli, A. Stefanucci, G. Macedonio, E. Novellino, S. Mirzaie, S. Dvorácskó, S. Carradori, L. Brunetti, G. Orlando, L. Menghini, C. Ferrante, L. Recinella, A. Chiavaroli, L. Leporini, A. Mollica, Int. J. Food Prop. 20 (2017), https://doi.org/10.1080/10942912.2017.1357127.
[15] F. Meyer, N. Ueberschaar, H.M. Dahse, Bioorg. Med. Chem. Lett. 23 (2013) 6043–6045.
[16] R.R. Soares, J.M.F. Silva, B.C. Carlos, et al., Bioorg. Med. Chem. Lett. 25 (2015) 2308–2313.
[17] E.B. Park, K.J. Kim, H.R. Jeong, et al., Bioorg. Med. Chem. Lett. 26 (2016) 5193–5197.
[18] L. Yang, P. Wang, J.F. Wu, Bioorg. Med. Chem. 24 (2016) 2125–2136.
[19] S.A. Carvalho, E.F. Silva, M.V.N. Souza, Bioorg. Med. Chem. Lett. 18 (2008) 538–541.
[20] X. Yu, P. Teng, Y.L. Zhang, Fitoterapia 127 (2018) 387–395.
[21] R.R. Pan, Z.Y. Feng, S.Y. Lu, et al., J. Anhui Agric. Sci. 4 (1982) 55–60.
[22] D. Patel, P. Kumari, N. Patel, Arch. Appl. Sci. Res. 2 (2010) 68.
[23] R. Mishra, I. Tomar, S. Singhal, K.K. Jha, Der. Pharm. Chem. 4 (2012) 489.
[24] A. Rao, A. Carbone, A. Chimirri, E. De Clercq, A.M. Monforte, P. Monforte, C. Pannecouque, M. Zappal'a, Farmaco 58 (2003) 115.
[25] A.K. Jain, A. Vaidya, V. Ravichandran, S.K. Kashaw, R.K. Agrawal, Bioorg. Med. Chem. 20 (2012) 3378.
[26] S.G. Kuçukguzel, E.E. Oruç, S. Rollas, F. Sahin, A. Ozbek, Eur. J. Med. Chem. 37 (2002) 197.
[27] F. Rahim, H. Ullah, M. Taha, A. Wadood, M.T. Javed, W. Rehman, M. Nawaz, M. Ashraf, M. Ali, M. Sajid, F. Ali, M.N. Khan, K.M. Khan, Bioorg. Chem. 68 (2016) 30–40.
[28] M. Taha, S.A.A. Shah, S. Imran, M. Afifi, S. Chigurupati, M. Selvaraj, F. Rahim, H. Ullah, K. Zaman, S. Vijayabalan, Bioorg. Chem. 75 (2017) 78–85.
[29] M. Taha, N.H. Ismail, H.M. Zaki, A. Wadood, E.H. Anouar, S. Imran, B.M. Yamin, F. Rahim, M. Ali, K.M. Khan, Bioorg. Chem. 75 (2017) 235–241.
[30] F. Rahim, K. Zaman, H. Ullah, M. Taha, A. Wadood, M.T. Javed, W. Rehman, M. Ashraf, R. Uddin, I. Uddin, H. Asghar, A.A. Khan, K.M. Khan, Bioorg. Chem. 63 (2015) 123–131.
[31] S. Shahid, M. Faisal, A. Saeed, S.A. Ghumro, H.R. El-Seedi, S. Rasheed, N. Abbas, F. Ali Larik, P.A. Channar, T.A. Fattah, Z. Ashraf, Z.A. Solangi, Curr. Org. Syn. 15

(2018) 1–18.
[32] (a) A.N. Barak, M. Taha, M. Gollapalli, F. Rahim, M. Ibrahim, A. Mosaddik, BMC Chem. 13 (2019) 14;
(b) F. Rahim, M. Taha, H. Ullah, A. Wadood, M. Nawaz, F. Khan, Z. Wahab, S.A.A. Shah, A.U. Rehman, A.N. Kawde, M. Gollapalli, Synthesis, in vitro urease inhibitory potential and molecular docking study of Benzimidazole analogues, Bioorg. Chem. 89 (2019) 103024;
(c) K. Zaman, F. Rahim, M. Taha, A. Wadood, S.A.A. Shah, M. Gollapalli, F. Ullah, Ashfaq Ahmed, Bioorg. Chem. 89 (2019) 102999;
(d) E.H. Anouar, M.E. Moustapha, M. Taha, M.H. Geesi, Z.R. Farag, F. Rahim, N.B. Almandil, R.K. Farooq, M. Nawaz, A. Mosaddik, Molecules 24 (2019) 963;
(e) M. Taha, F. Rahim, M. Ali, M.N. Khan, M.A. Alqahtani, Y.A. Bamarouf, M. Gollapalli, R.K. Farooq, S.A.A. Shah, Q.U. Ahmed, Z.A. Zakaria, Molecules 24 (2019) 1528;
(f) N.B. Almandil, M. Taha, F. Rahim, A. Wadood, S. Imran, M.A. Alqahtani, Y.A. Bamarouf, M. Ibrahim, A. Mosaddik, M. Gollapalli, Bioorg. Chem. 85 (2019) 109–116.
[33] M. Taha, N.H. Ismail, S. Lalani, M.Q. Fatmi, A. Wahab, S. Siddiqui, K.M. Khan, S. Imran, M.I. Choudhary, Eur. J. Med. Chem. 92 (2015) 387–400.
[34] L.K. Williams, X. Zhang, S. Caner, C. Tysoe, N.T. Nguyen, J. Wicki, D.E. Williams, Nature Chem. Biol. 11 (2015) 691–696.
[35] Dassault Systèmes BIOVIA, [Discovery Studio v18.1.100.11], Dassault Systèmes, San Diego, 2018.
[36] K. Oliver, S. Thomas, E. Thomas, J. Chem. Inf. Model 49 (2009) 84–96.
[37] Molecular Operating Environment (MOE), 2016.08, Chemical Computing Group Inc., 1010 Sherbrooke St. West, Suite #910, Montreal, QC, Canada, H3A 2R7, 2016.
[38] M.W. Weatherburn, Phenol-hypochlorite reaction for determination of ammonia, Anal. Chem. 39 (1967) 971.
[39] a) M. Taha, N.H. Ismail, S. Imran, A. Wadood, F. Rahim, K.M. Khan, M. Riaz, Bioorg. Chem. 66 (2016) 80;
b) M. Taha, N.H. Ismail, A. Khan, S.A.A. Shah, A. Anwar, S.A. Halim, M.Q. Fatmi, S. Imran, F. Rahim, K.M. Khan, Bioorg. Med. Chem. Lett. 25 (2015) 3285.
[40] S.P. Loh, O. Hadira, J. Nature 17 (2011) 77–86.
[41] S. Imran, M. Taha, M. Selvaraj, N.H. Ismail, S. Chigurupati, J.I. Mohammad, Bioorg. Chem. 73 (2017) 121.